AgriEngineering

MDPI

Article

Cloud-Enabled Multi-Axis Soilless Clinostat for Earth-Based Simulation of Partial Gravity and Light Interaction in Seedling Tropisms

Christian Rae Cacayurin [1], Juan Carlos De Chavez [1], Mariah Christa Lansangan [1], Chrischell Lucas [1], Justine Joseph Villanueva [1], R-Jay Relano [1,2], Leone Ermes Romano [3] and Ronnie Concepcion II [1,2,*]

[1] Department of Manufacturing Engineering and Management, De La Salle University, Manila 1004, Philippines; cacayurinrae@gmail.com (C.R.C.); juancarlosdechavez@gmail.com (J.C.D.C.); mariahcglansangan@gmail.com (M.C.L.); chrischell_lucas@dlsu.edu.ph (C.L.); justine_villanueva@dlsu.edu.ph (J.J.V.); r-jay_relano@dlsu.edu.ph (R.-J.R.)
[2] Center for Engineering and Sustainability Development Research, De La Salle University, Manila 1004, Philippines
[3] Department of Agricultural Sciences, University of Napoli Federico II, 80055 Portici, Italy; leoneermes.romano@unina.it
* Correspondence: ronnie.concepcion@dlsu.edu.ph

Abstract

Understanding the combined gravi-phototropic behavior of plants is essential for space agriculture. Existing single-axis clinostats and gel-based grow media provide limited simulation fidelity. This study developed a Cloud-enabled triple-axis clinostat with built-in automated aeroponic and artificial photosynthetic lighting systems for Earth-based simulation under Martian gravity ranging from 0.35 to 0.4 *g*. Finite element analysis validated the stability and reliability of the acrylic and stainless steel rotating platform based on stress, strain, and thermal simulation tests. Arduino UNO microcontrollers were used to acquire and process sensor data to activate clinorotation and controlled environment systems. An Arduino ESP32 transmits grow chamber temperature, humidity, moisture, light intensity, and gravity sensor data to ThingSpeak and the Create IoT online platform for seamless monitoring and storage of enviro-physical data. The developed system can generate 0.252–0.460 *g* that suits the target Martian gravity. The combined gravi-phototropic tests confirmed that maize seedlings exposed to partial gravity and grown using the aeroponic approach have a shoot system growth driven by light availability (395–400 μmol/m^2/s) across the partial gravity extremes. Root elongation is more responsive to gravity increase under higher partial gravity (0.375–0.4 *g*) even with low light availability. The developed soilless clinostat technology offers a scalable tool for simulating other high-value crops aside from maize.

Keywords: automated farming; controlled environment agriculture; gravitropism; microenvironment; rotating platform; space agriculture

check for updates

Academic Editor: Eugenio Cavallo

Received: 14 June 2025
Revised: 1 August 2025
Accepted: 4 August 2025
Published: 12 August 2025

Citation: Cacayurin, C.R.; De Chavez, J.C.; Lansangan, M.C.; Lucas, C.; Villanueva, J.J.; Relano, R.-J.; Romano, L.E.; Concepcion, R., II. Cloud-Enabled Multi-Axis Soilless Clinostat for Earth-Based Simulation of Partial Gravity and Light Interaction in Seedling Tropisms. *AgriEngineering* **2025**, *7*, 261. https://doi.org/10.3390/agriengineering7080261

Copyright: © 2025 by the authors. Licensee MDPI, Basel, Switzerland. This article is an open access article distributed under the terms and conditions of the Creative Commons Attribution (CC BY) license (https://creativecommons.org/licenses/by/4.0/).

1. Introduction

Understanding of plant tropisms in non-terrestrial environments is essential for the future of both space agriculture and growing plants in extraterrestrial environments, as well as basic plant physiology. As human explorations progress out of low-Earth orbit to the surfaces of the moon and Mars, validated plant-based life support systems will be critical for the sustainable production of food and bioregenerative systems. Tropism, or the

directional growth responses to environmental stimuli, including gravity (gravitropism) and light (phototropism), is a key determinant of plant form, resource acquisition, and developmental plasticity in a variable-gravity environment [1,2].

Gravity exerts a strong effect on plant structure and growth by regulating auxin distribution and its activation of distinct gene networks in gravisensing tissues, including root columella cells and shoot endodermis [3,4]. This hormone-regulated polarity fuels the penetration of roots and the elevation of shoots, both essential for space orientation occupied in terrestrial plants. However, these processes are greatly affected by microgravity. For example, it was found that root bending in response to light could only be detected in *Arabidopsis* seedlings in the absence of gravity, vanishing even at 0.1 *g*, indicating that terrestrial gravity masks subtle phototropic responses [5]. The relative growth rate of *Wolffia globosa* under simulated microgravity was significantly lower than in a 1 *g* environment [6]. Likewise, phototropic curvature in roots and hypocotyls decreases sharply from 0.1 *g* to 0.3 *g* [5], emphasizing the need for partial-gravity simulations. Generally, single-axis clinostats are used to simulate partial gravity on Earth, but they only average the gravity vector and do not create partial gravity conditions. Higher-order systems such as Random Positioning Machines (RPMs) and dual-axis clinostats increase simulation fidelity at the cost of mechanical complexity and limited capability for environmental modulation in real time [7,8]. A recent study on the optimization of 3D clinostats has shown that the ratio between the angular velocities of the outer axis to the inner axis (4:1.8) is key to establishing homogeneous simulated gravity fields [9]. Despite these advancements, existing approaches generally suffer from limited adaptability for joint light modulation and time-resolved data acquisition.

Recent experiments on the International Space Station (ISS) with the European Modular Cultivation System (EMCS) have revealed a new blue-light receive-positive phototropic response in roots of *Arabidopsis* growing under microgravity that is a responsiveness masked by the stronger gravitropic response predominant in plants growing under Earth gravity. This response was reduced at 0.1 *g* and not detectable at higher gravity levels, thus demonstrating a threshold effect [10]. In addition, red-light pre-treatment increased blue-light phototropism, suggesting a complicated, additive relationship between light quality and tropic signaling pathways [10]. Furthermore, differences between terrestrial and space-synchronized phototropic responses can occur from the irregularity of photoperiods, unevenness of light sources in seedling cassettes, as well as traditional cold stowage and seed viability limitations. Light leakage and long storage times of seeds have compromised the integrity and collection of data for many ISS experiments, including the work carried out in the TROPI-1 and TROPI-2 studies [10]. These results agree with later EMCS results indicating enhanced blue-light phototropism in *Arabidopsis* roots grown in microgravity when red was added, which also reasoned that gravitropic signals were suppressed [10].

Soilless systems like hydroponics and aeroponics provide accurate nutrient and water delivery, pH control, and reduced microbial contamination, which is advantageous for controlled studies of tropic responses [11–13]. Such systems permit consistent environmental control over the dynamics of the root zone critical for gravity-dependent investigations. Soil is impractical in microgravity due to risks of particulate dispersal and behavior of voids in less than 1 *g*; liquid- or mist-based soilless methods are preferred for reliability and containment [12]. But they are not easily integrated with dynamic simulation systems such as clinostats and bioreactors, with limitations in spatial footprint, liquid redistribution under rotation, as well as risk of fluid leakage [11]. It has been demonstrated that various nutrient media parameters such as water transport time (WAT), air-filled porosity (AFP), and active surface ratio (ASR) need to be optimized to create healthy root environments and

gas exchange rates [14]. Utilizing hydroponics for growth during space-based experiments is now validated by lettuce grown aboard the Chinese Tiangong II station under orbital conditions; it showed structural integrity, consistent leaf morphology, and productivity across growth states [13]. These media also proved adaptable to duckweed species, including both *Lemna* and *Wolffia*, which were grown in simplified liquid media systems and tracked for morphology and growth parameters with automated platforms [15].

Cloud-based sensor networks can continuously measure temperature, relative humidity, light spectra, nutrient flow, and growth metrics, and a subset of platforms can even implement AI-based alerts or adaptive controls [16]. These technologies reduce human errors, enable remote control of experiments, and will add scalability to the laboratory and orbital farming systems. The use of a machine learning-based image segmentation software called Ilastik® was suggested to automate the evaluation of morphological traits in *Lemnaceae*, including *Wolffia globosa* and *Lemna minor*, obtaining a correlation coefficient of 0.99 in comparison with conventional measurements [15]. *Wolffia globosa* displayed substantial morphological plasticity and differences in attributed ratio of gravitational growth rate when grown in perceived microgravity [6]. *Arabidopsis thaliana* in microgravity conditions unmasked an inhibited normal root phototropic response under 1 *g*, pointing toward the importance of coordinating stimulus simulation over time [10].

Despite these technological advancements, many existing studies rely on static light setups and single-axis clinostats that provide limited simulation fidelity. These systems typically lack spatially resolved stimulus control and do not support real-time environmental feedback, thus constraining the exploration of dynamic plant responses to simultaneous stimuli [7,17,18]. As a result, the interaction between gravitational and photic stimuli remains underexplored. For instance, *Wolffia globosa* has shown significant morphological variability and differences in relative growth rate (RGR) under simulated microgravity conditions; however, quantitative data capturing the interaction of light directionality and altered gravity are still emerging [6]. Similar findings have been reported in *Arabidopsis thaliana*, where microgravity conditions revealed atypical root phototropic responses otherwise suppressed under 1 *g*, emphasizing the need for synchronized stimulus simulation [10]. Additionally, a recent transcriptomic study in rice roots grown under clinostat-induced microgravity revealed rapid modulation of auxin-related gene expression, particularly heat shock protein (HSP) genes, suggesting early molecular responsiveness to gravity vector changes and reinforcing the need for integrated light-gravity experimentation [19].

To address these limitations, this study developed a Cloud-enabled multi-axis soilless clinostat for Earth-based simulation of partial gravity and light interaction in seedling tropisms. This system has an integrated soilless cultivation system to study plant seedling tropisms under Earth-simulated partial gravity and controlled lighting environments. It involves designing the rotating platform by incorporating static and dynamic simulation analysis and manufacturing techniques for fabrication; automating the clinostat rotation using off-the-shelf Arduino boards, which enables the end users to adjust the motor speed within the specified thresholds for Mars surface's partial gravity (0.35 *g*–0.40 *g*); configuring the Cloud-based IoT network through ThingSpeak for continuous monitoring of enviro-physical parameters inside the grow chamber; and automating the aeroponic fertigation system for nutrient delivery to seedling root systems and a photoperiod-based lighting system to stimulate plant growth. The system should operate continuously for one week, constituting half of the experimental duration.

This study mainly contributes the following:

(1) Development of an Earth-based simulated partial gravity platform with seamless wireless environmental data transmission and monitoring and integrated aeroponic and lighting systems to support crop growth;

(2) Elucidation of gravitropic and phototropic responses of maize seedlings under partial gravity environment. This development helps in preparing food production systems and techniques for astronauts and improving technologies linked with bioregenerative life support systems in space.

2. Materials and Methods

This study involves five major developmental phases, namely (1) designing and rapid prototyping of clinostat; (2) automating of 3-axis clinostat rotation; (3) embedding of Cloud-based IoT network for monitoring enviro-physical parameters inside the grow chamber; (4) automation of fertigation and lighting systems; and (5) initial test cultivation by exposing corn seeds in Martian gravity and varied light intensity (Figure 1).

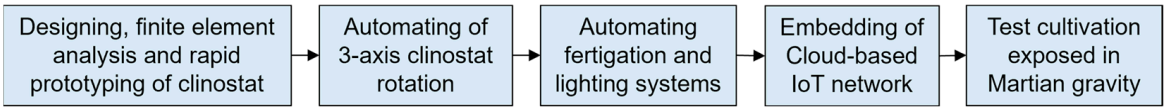


Figure 1. Step-by-step process flow of developing Cloud-enabled multi-axis soilless clinostat for Earth-based simulation of partial gravity and light interaction in seedling tropisms.

2.1. Designing and Rapid Prototyping of Clinostat

The clinostat platform was designed using SolidWorks 2024 software, which includes the 3D model of the grow chamber. The design of the grow chamber is divided into three sectors. The upper (for plant shoot zone) and outer (for plant root zone) sectors of the grow chamber are for the plant chamber, while the middle sector is for the fertigation system (Figure 2). The grow chamber is 304 mm × 304 mm × 304 mm, considering there is a maximum of 36 seedlings to be cultivated inside. The design of the clinostat was based on standard protocol [7]. Using SolidWorks 2024 software, a motion analysis of the rotating platform design was performed, considering the weight or load range of the grow chamber to be 5–10 kg, accounting for the combined weight of the upper growth chamber, seedlings, nutrient system, and sensors, which resulted in power stability within 5 s. This load specification ensures mechanical stability and minimal deformation under operating conditions, as verified through von Mises stress and equivalent strain simulations. Finite element analysis (FEA) was employed to characterize the static stress, static strain, and dynamic thermal performance of the clinostat. This is necessary to analyze the potential stress and deformation patterns under the gravity condition, as well as the fluctuating temperature and heat transfer due to active motors. The next step was the development of the prototype using rapid prototyping. In this procedure, acrylic and metal (stainless steel) fabrication were performed. A transparent acrylic sheet was used in constructing the crop growth chamber at the center of the platform. One layer of aluminum foil was covered in the internal wall of the growth chamber to avoid external light reaching the interior during the light-on and dark periods. Stainless steel was used to manufacture the frames of the clinostat. All acrylic and metal sheets are 3 mm thick. A laser cutter was used to precisely cut the acrylic based on the design, an acrylic solvent adhesive was used to join the faces of acrylic cutouts, and an edge finisher was applied to finish the grow chamber having smooth surfaces. The stainless steel fabrication involves using a computer numerical control (CNC) laser cutter and drill press for the holes, welding joints, and sanding and polishing for finishing. Passive aeration in the upper growth chamber was facilitated by an open headspace and the intermittent operation of the misting system, which generated fine droplets around 20–50 μm that increased the surface area at the root–air interface. The droplet-based delivery provided temporary film-free exposure of roots to air between pulses, which simulates oxygen exchange conditions similar to dynamic aeroponic systems. While the developed clinostat has no dedicated gas control system

installed, the grow chamber design allowed for convective mixing and diffusion of gases between the root zone and the chamber air volume (Figure 2b,c).

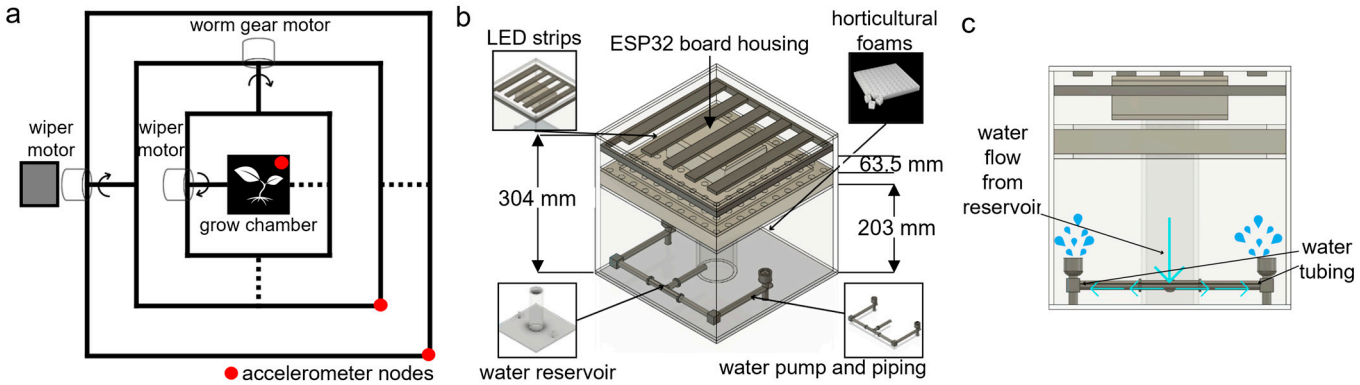


Figure 2. (**a**) Top view line structure of the 3-axis clinostat; (**b**) placement of lighting and fertigation components; and (**c**) direction of water flow from reservoir to the root zone inside the grow chamber.

2.2. Automating of 3-Axis Clinostat Rotation

The orientation of the developed clinostat in three dimensions can be shown visually with a three-axis rotation (Figure 2a). The outermost, center, and innermost perpendicular axes of the clinostat schematic each indicate a distinct rotational direction (Figure 2a). The center axis spins around the vertical axis through a worm gear motor, the innermost axis rotates around the axis perpendicular to the center axis (horizontal), and the outermost axis rotates around the horizontal axis. This configuration allows quick and stable transition from simulated rotation or gravity to another. Three controlled motors are responsible for the independent rotation of each axis with rotation based on the gravitational force conversion (1), Euclidean norm vector magnitude (2), angular velocity conversion (3), and radial acceleration formula (4), where g is the Earth's gravitational constant, with a value of 9.81 m/s^2; g_{target} is the target g-value; g_{total} is the magnitude g-value considering the three axis gravity values g_x, g_y, and g_z for 3-axis rotation; ω_i is the angular velocity (rad/s) of the central axis (grow chamber); N_i is the rotational speed of each rotating axis; g_i is the centripetal acceleration of an axis (m/s^2); and r is the radius of rotation (m) that is 0.5 m in this case.

$$g_{total} = g_{target} \times g \tag{1}$$

$$g_{total} = \sqrt{{g_x}^2 + {g_y}^2 + {g_z}^2} \tag{2}$$

$$\omega_i = \frac{2\pi N_i}{60} \tag{3}$$

$$g_i = {\omega_i}^2 r \tag{4}$$

In this study, the target g-force generated by the clinostat is 0.35 g to 0.4 g. To achieve this, the innermost, middle, and outermost axes were configured to rotate between 11 and 13 rpm, 23 and 24 rpm, and 19 and 20 rpm, respectively. The outermost and middle axes are powered by a 30 W wiper motor, which has a maximum of 50 rpm as its speed with no load, whilst the innermost axis is powered by a 12 V DC worm gear motor with a maximum no-load speed of 80 rpm (Figure 2a). To control all three motors, two L298N DC dual H-bridge stepper motor driver board modules were utilized. Through the motor driver, the motors were automatically set to the ideal rotation speed needed to achieve a gravity of 0.35 g to 0.40 g. A 12 V Pulse Width Modulator (PWM) motor speed controller regulator was also added per axis for the motors to stop gradually, which will reduce the wear and tear of the motors. With this, 6205ZZ and 6206ZZ bearings were utilized to reduce the friction

and allow the rotation of the clinostat to be smooth, reducing the amount of energy needed to be consumed. This ensures that the rotating shaft maintains a correct position while the clinostat is running. On the other hand, the wires used for the Arduino UNO-based circuit go through all the axes, and so as a consideration (Figure 3), three slip rings with six channels were used to allow organized continuous rotation of these wires throughout the clinostat. To validate the *g*-value inside the chassis, MPU-6050 accelerometer was used to obtain the linear acceleration and angular velocity in x, y, and z following (1) to (4), where it was embedded in Arduino UNO boards using the C++ programming language for automated computation, resulting in smooth and stable rotation. One accelerometer was placed for each axis (Figure 2a). Twenty varied test sequences of different combinations of inner-, middle-, and outer-axis rotational speeds were configured, and the resulting *g*-value were measured to verify the reliability of the clinorotation. This was performed for 16 h per combination.

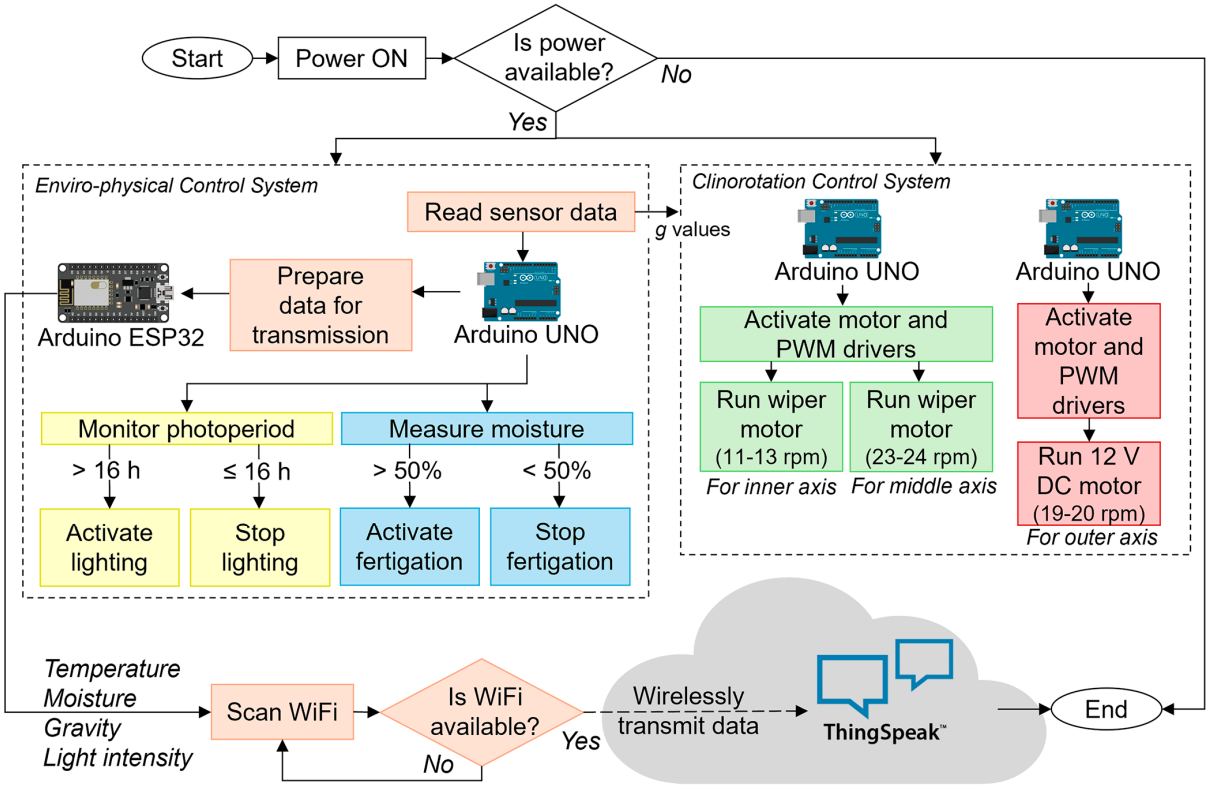


Figure 3. Sensor data flow and Cloud-based IoT network infrastructure of the developed soilless clinostat platform. The control system includes an Arduino UNO R3 microcontroller (ATmega328P, 5 V, 16 MHz), ESP32 WiFi module (dual-core, 2.4 GHz), DHT22 temperature–humidity sensor (±0.5 °C, ±2% RH), capacitive moisture sensor (v1.2), PPFD sensor, 5 V relay module, and 12 V diaphragm pump (350 mL/min). Environmental data are monitored in real time and transmitted to the Arduino IoT Cloud via the ESP32 module. The RGBW LED strips (SMD 5050, 60 LEDs/m) are also controlled through a timed relay circuit for photoperiod regulation.

2.3. Automating Fertigation and Lighting Systems

Two cultivation-related biosystems were developed, namely fertigation and lighting systems. The fertigation system exhibited automated delivery of nutrient-rich water to the seedling and root zone through pulse misting with a 1 L reservoir placed at the center (Figure 2b,c). To achieve seamless fertigation, an Arduino UNO (ATmega328P, 5 V logic, 16 MHz) microcontroller board was used, to which a moisture sensor placed inside the root zone of the grow chamber was connected (Figure 3). Since the current study explores the possibility of germinating seeds under Martian gravity through a soilless approach, the sys-

tem has been configured to activate a relay switch connected to the misting cooling module with a 12 V mini-submersible water pump (flow rate of approximately 350 mL/min) if the measured moisture within the root zone is less than 50%, and it deactivates when it is above 50% to avoid overwatering that might cause the formation of root mold. Once activated, the water flows from the reservoir to the pumping station in both the left and right directions (Figure 2c). After it reaches the pumping station, the water continues flowing and is released through the sprinkler to water the root zone of the plant chamber, and this process repeats every 30 min. The second part is the horticultural foam (Oasis® Grower Solutions, Kent, OH, USA) section, which is composed of one chamber and 36 seedlings. The nutrient solution in the 1 L water reservoir has dissolved 10 g of NPK 14-14-14 powder (Harvester, Birmingham, UK) [20]. The current platform design does not incorporate an active drainage system. Instead, the misting system operates in short-duration, low-volume pulses (2 s every 15 min) that were initially optimized to prevent waterlogging and maintain a moist yet aerated root zone. The horticultural foam medium has sufficient porosity to temporarily retain mist without saturating, and excess liquid is absorbed by the foam or gradually evaporates within the sealed chamber. This minimalist design was opted for as it is appropriate for short-term seedling studies and enables operation in closed environments without the complexity of drainage plumbing. However, for longer-term plant cultivation or biomass production, future platform upgrades may incorporate a passive or active drainage line to prevent moisture accumulation. The automated lighting system is composed of photosynthetic artificial light, mainly a pure red (660 nm wavelength, 2000–3000 K color temperature); pure blue (450 nm wavelength, 5000–6500 K color temperature), red, blue, and green (RGB) (530–630 nm wavelength, 4000–6000 K color temperature); and white (400–700 nm wavelength, 2700–6500 K color temperature) LED strip (RGB SMD 5050 strip with 60 LEDs/m and 391 $\pm$ 9.460 $\mu mol/m^2/s$ light intensity using a photosynthetic photon flux density sensor) spectrum arranged in a serpentine fashion and attached at the ceiling of the upper chamber (Figure 2b). In this study, there is no light intensity control because there is only a small space margin for the growing region in the platform. The pure red spectrum promotes flowering and fruiting. The pure blue spectrum supports vegetative growth. RGB of equal distribution (1 R:1 G:1 B) is for multi-spectral compositive light that mimics natural sunlight. White light fills gaps of the other spectra that includes some far-red or near-ultraviolet spectra. For the cultivation experiment, combined red, blue, and green LEDs were utilized. The lighting system is activated every 16 h (photoperiod) at the start of turning ON the main switch of the clinostat platform through the built-in timer programmed through the Arduino UNO microcontroller (Figure 3). The automated lighting system rather refers to the activation of the photoperiod and maintaining it for up to 16 h.

The microcontrollers were programmed using the Arduino IDE (v1.8.x), with environmental sensors polled every 5 min. Sensor data and execution status of misting and lighting routines were transmitted via WiFi to ThingSpeak Cloud, where values were stored and visualized on a real-time dashboard. This platform enabled both monitoring and timestamped logging of command executions, such as mist activation cycles and light ON/OFF periods, thereby supporting traceability and experimental validation. A representative sample of the recorded data and interface is shown in the succeeding section.

2.4. Embedding of Cloud-Based IoT Network

The entire clinostat system is connected to a Cloud-based IoT network to support the seamless virtual monitoring of the end user and allows historical controlled environment data to be recorded for future analysis. Provided in Sections 2.2 and 2.3 is the same Arduino UNO board (ATmega328P, 5 V logic, 16 MHz) that is cascaded with an ESP32 NodeMCU

WiFi (dual-core Xtensa® 32-bit LX6, 2.4 GHz, 3.3 V logic) microcontroller breakout board for wirelessly transmitting temperature and humidity (DHT11, accuracy: ±0.5 °C, ±2% RH), Arduino-based capacitive moisture, gravity (MPU-6050 accelerometer), and Grove light intensity data inside the grow chamber to ThingSpeak and the Create IoT online platform (Figure 3). The microcontroller allowed acquisition and transmission of sensor data per minute; that is a data rate of 16.667 mHz.

2.5. Test Cultivation and Statistical Analysis

Two cultivation treatments were performed: control treatment (CT) and partial gravity (PG) treatment. To verify the reliability of the developed soilless clinostat in growing seedlings under partial gravity, triplicate experiments (36 seeds/trial × 3 trials = 108 seeds) were performed with gravity maintained between 0.35 *g* and 0.4 *g* for a 16 h photoperiod under a photosynthetic light spectrum. Each trial ran for 7 consecutive days each. The measured total volume of nutrient-rich water per day was 40 mL. The misting system dispensed a total of approximately 40 mL of nutrient-rich water per day, as measured from the reservoir. This value includes both plant uptake and evaporative loss, as no drainage system was present. Horticultural foams were placed at the upper chamber, forming a fixed layer of grow substrate. Waxy corn or Lagkitan (IPB var 6) is the variety of *Zea mays* L. provided by the Bureau of Plant Industry, Manila, Philippines. The only difference of CT from PG is that there is no manifested axis rotation, resulting in natural 1 *g* exposure. At the end of each cultivation trial, the root shoot and root length were measured with a laboratory metric ruler having 1 mm resolution. The root-to-shoot ratio was computed by dividing the root and shoot lengths. To statistically determine the difference between the means of CT- and PG-generated plant parameters, a paired *t*-test was performed with a 95% confidence level ($\alpha = 0.05$) using Minitab v.18 software. All surface graphs showing gravitropism and phototropism were generated using Minitab v.18 software with the distance method, having a distance power of 2 as the interpolation method.

3. Results

3.1. Finite Element Analysis and Fabricated Clinostat

The final design of the clinostat with a grow chamber used acrylic and stainless steel materials to fully support the gravitational force during rotation and the load due to water in the water reservoir (Figure 4a). The fabricated clinostat completely resembled the design (Figure 4b). The stress and strain analysis in FEA involves the assessment of the location of mechanical stress and strain within a given structure under the influence of gravity (Figure 4c,d). The analysis of stress and strain distribution in the frame and other components of a three-axis clinostat was conducted by examining the centrifugal forces created by the rotation of the clinostat. The minimum and maximum for von Mises stress is 209.32 N/m^2 and 3.304e^6 N/m^2, respectively, where all the mildly strained areas of the platform are the connecting joints (Figure 4c). The minimum and maximum for equivalent strain are 6.760e^{-9} and 1.463e^{-5}, respectively, where potential deformation due to load may also happen along connecting joints (Figure 4d). Based on these analyses, it is found that there is correct distribution of stress on the platform, and it is ensured that material deformation stays within the safe limits under expected loading. There were no indications of excessive strain that could compromise the precision and stability of the clinostat during rotation. The thermal analysis confirmed the localized heating at the motor junctions (≈ 48 °C hottest possible), not affecting the grow chamber (ranging from 24 °C to 30 °C) (Figure 4d). There is sufficient thermal dissipation, not affecting plant growth and electronic component reliability. The chamber was mechanically fastened to the rotating frame using custom-designed aluminum brackets and non-slip rubber washers to

ensure stability during multi-axis movement. Structural integrity was validated using static and dynamic stress analysis in ANSYS 2024 R2 (Figure 4c–e). To ensure smooth motion, each of the three stepper motors was controlled via a microstepping driver configured to 1/16 microsteps, reducing vibration and ensuring near-continuous rotational movement. These measures were critical in avoiding mechanical stress on to the seed tissues. Hence, the clinostat design is applicable for fabrication.

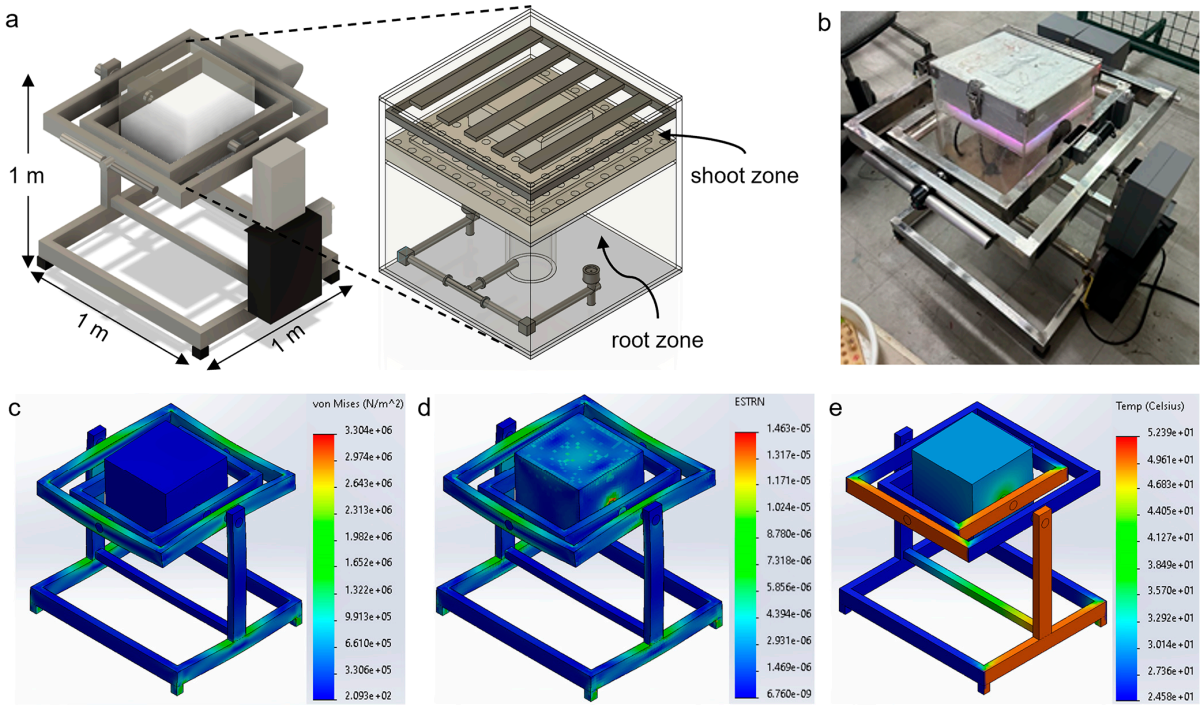


Figure 4. (**a**) Final grow chamber and clinostat platform design with mechanical fastening via rubber-dampened aluminum brackets; (**b**) fabricated clinostat with integrated vibration control; and (**c**) von Mises static stress, (**d**) equivalent static strain (ESTRN), and (**e**) dynamic thermal characterization of the platform in ANSYS 2024 R2. Although simulations confirmed low mechanical stress under load, additional smoothness control was implemented via motor drivers and acceleration ramping to protect photosynthetic tissues during rotation.

3.2. Clinorotation

The developed clinostat replicates partial gravity conditions by rotating the grow chamber containing maize seedlings along with many axes. Based on the 20-run reliability test, the fabricated clinostat can operate at target Martian gravity (0.35 g to 0.4 g) (Figure 5a). It indicates that an average of 18 rpm across all axes effectively simulates the target partial gravity range. To operate at the smoothest approximation of partial gravity, it is recommended to configure the motors to 11 rpm for the inner axis, 23 rpm for the middle axis, and 20 rpm for the outer axis, through a potentiometer connected to the PWM motor driver module. Based on actual tests for maintaining gravity to 0.356 $\pm$ 0.010 g, on average, the inner, middle, and outer axes were operated at 10.850 $\pm$ 0.450 g, 23.450 $\pm$ 0.750 g and 21.100 $\pm$ 1.300 g, respectively. This resulted in a very low rotational error of 2.921%, which makes the fabricated clinostat system recommendable for crop cultivation experiments. Hence, the developed clinostat can generate partial gravity from 0.252 g to 0.460 g, and proper configuration of the rotational speed of each axis should be applied to attain the target gravitational force inside the grow chamber.

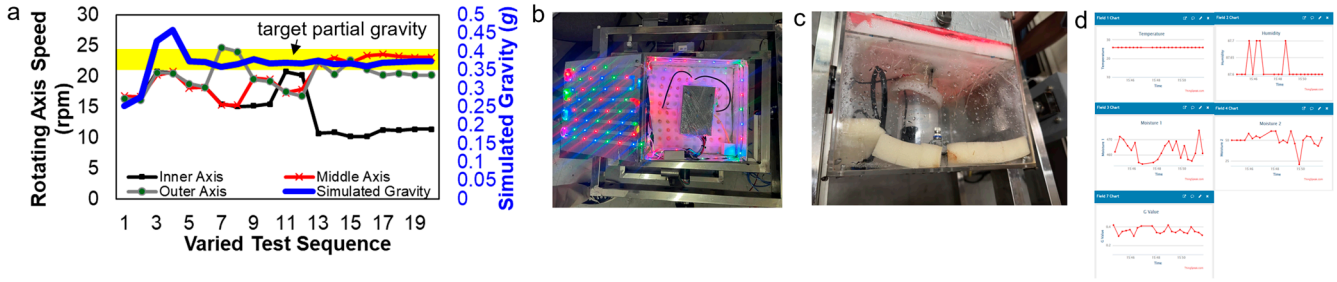


Figure 5. (**a**) Twenty runs of the reliability test for the developed clinostat with varied values of axis speeds. (**b**) Internal view of the upper growth chamber with the acrylic lid open, showing the ceiling-mounted RGBW LED strip and plant support tray. (**c**) View of the lower chamber during demonstration, with foam material temporarily placed to visually highlight the position and function of the aeroponic misting zone. In the actual experiment, this foam was not present in the lower chamber and does not serve a functional role in the fertigation process. (**d**) Screenshot of the ThingSpeak IoT dashboard showing real-time trend graphs generated from Cloud-logged sensor data. This panel is included not to show specific data values but to demonstrate the functionality and integration of a working Cloud-based monitoring system. Clear temporal trends in light, misting, and environmental conditions confirm active data transmission from the ESP32 module.

3.3. Automated Aeroponic Fertigation and Lighting Systems and Cloud IoT System

The operational lighting and aeroponic fertigation systems fit for cultivating seedlings are shown in Figure 5b,c. These two important controlled environment systems are controlled by the Arduino UNO microcontroller, where the lighting system turns on for 16 h and off for 8 h, and the fertigation system activates the misting operation for 30 min whenever the moisture inside the root zone is below 50%. The sprinklers spread water onto the horticultural foam upward to deliver water to embedded seeds and roots whenever they germinate. Horticultural foam is a porous, synthetic substrate that is commonly used for seed germination and hydroponic applications [11]. In this study, it was employed as the growth medium in the upper chamber. It retains moisture through capillary action and offers structural support for emerging roots so the resulting root would be upright [13]. Its relatively slow water absorption rate compared to liquid or gel-based media may delay initial hydration, which may potentially bias early root elongation measurements; its form-stability, low microbial contamination risk, and compatibility with aeroponic misting systems make it the most suitable grow medium for this experimental platform [11]. The crop grow chamber in Figure 5c shows the accumulated water due to misting. Moisture, temperature and humidity, light intensity, and gravity sensor data were streamed to the Arduino IoT Cloud platform for virtual monitoring and historical data storage (Figure 5d in mobile phone view). This emphasized that the developed fertigation and lighting systems can support operation inside a microenvironment for plant growth automatically.

3.4. Synthesis of Partial Gravity and Light Tropisms

After conducting three trials for CT and PG treatments, maize seeds grew differently, with the control environment (1 *g*) inducing more growth when provided with the same lighting spectrum and intensity condition than the Martian gravity-treated seeds (Figure 6). Based on measured root length, CT seeds grew 241.744% longer than PG seeds (43 ± 68 mm) with a range of 103 ± 65 mm (Figure 6b). CT-treated seeds resulted in 256.864% longer shoots (158 ± 114 mm) than the PG-treated seeds (61 ± 43 mm) (Figure 6c). In terms of root-to-shoot ratio, PG-treated seeds exhibited one 115.707% higher (0.086 ± 0.143) than CT-treated seeds (0.075 ± 0.068) (Figure 6d). Based on visual observation, the CT shoots exhibited more prominent vertical growth under the Earth's gravity, which indicates positive gravitropic response, while there is no discernible pattern in the direction of

PG shoots, suggesting the suppression of normal gravitropic signaling due to triple-axis rotation. The stability of gravity exposure inside the grow chamber together with the root zone temperature and humidity during cultivation are shown in Figure 6e–g. The internal chamber temperature was continuously monitored using a DHT22 sensor connected to the Arduino data logger. Throughout all trials, the root zone temperature was maintained at 25 ± 1.5 °C, with no statistically significant differences observed between experimental runs (Figure 6f). The ambient room was air-conditioned and maintained at 24–26 °C to minimize thermal variation. These controls ensured that observed gravitropic responses were not confounded by thermal gradients. Based on measured root and shoot lengths, there is no clear trend when they will grow faster with the combined impacts of gravity and light intensity (Figure 6h,i). Based on PG treatment, root length grew longer at the lower end of used light intensity (385 µmol/m^2/s) and high end of partial gravity (0.375 *g* to 0.4 *g*). This proves that maize seed roots respond to stronger partial gravity due to improved mechanostimulation that results in root elongation. Shoot length increases at the higher end of light intensity (395–400 µmol/m^2/s) for both partial gravity extremes (0.350 *g* and 0.400 *g*). This proves that the maize shoot system is driven more by the light signal and is dominant over gravitropic response in the partial gravity range. Paired *t*-tests confirmed that the mean root and shoot lengths significantly differed between the CT and PG treatments. For root length, the difference was highly significant ($p = 0.001$, $t = 5.70$), and for shoot length, the difference was also significant ($p = 0.003$, $t = 5.21$). The root-to-shoot ratio of both CT and PG treatments are not statistically and significantly different ($p = 0.560$, $t = -0.590$).

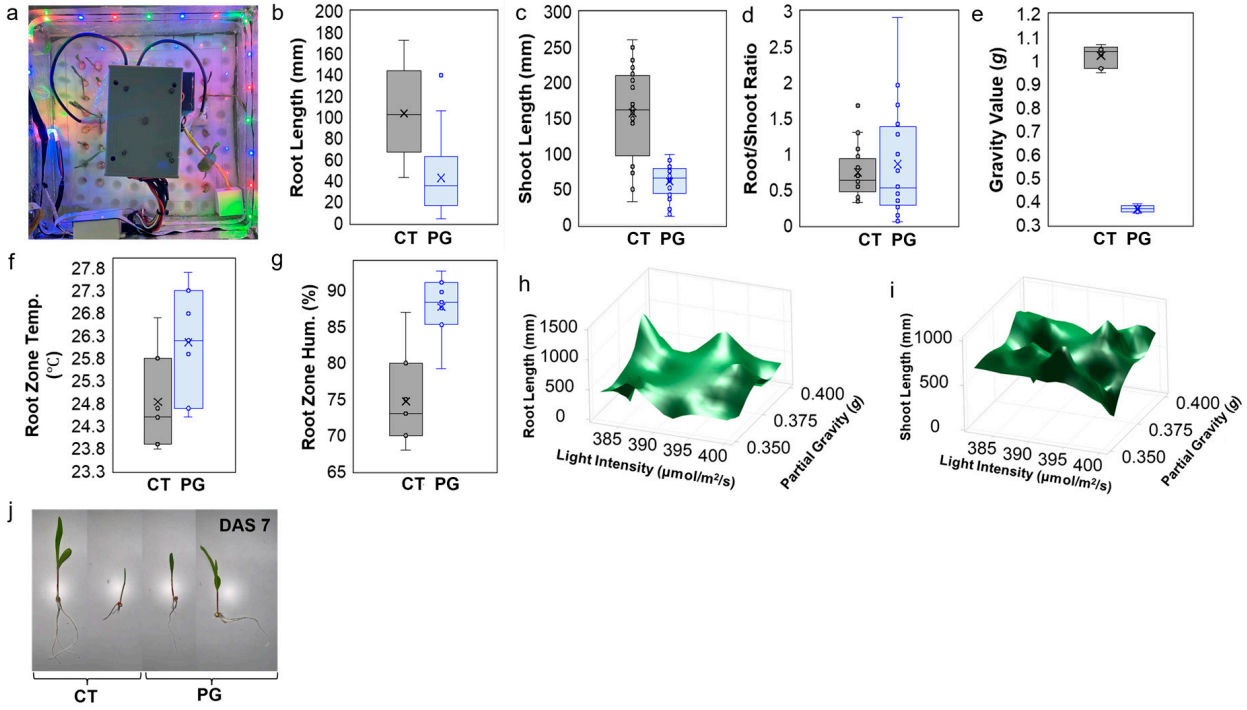


Figure 6. (**a**) Sample grown maize seedlings inside the fabricated grow chamber after 7 days under partial gravity (top view); comparisons of control treatment (CT) and partial gravity (PG)-treated maize seedlings for triplicates based on (**b**) root length, (**c**) shoot length, and (**d**) root/shoot ratio; measured (**e**) gravity, (**f**) root zone temperature, and (**g**) root zone humidity inside the chamber during cultivation; and (**h**) root and (**i**) shoot dynamics in relation to gravity and light intensity exposure. (**j**) Sample CT and PG-treated seedlings on the 7th day after sowing (DAS). Note: Surface plots are interpolated visualizations based on seedling observations and are meant to highlight directional trends, not precise biological gradients. Apparent sharp peaks may result from local data variation amplified by the interpolation algorithm.

4. Discussion

Space analog environments are engineered spaces, usually enclosed and with a feedback system, to mimic the environment in space. Though there are existing larger space analogs such as the Mars Desert Research Station (MDRS) in Utah and the Hawaii Space Exploration Analog and Simulation (HI-SEAS) [21,22], their focus is more on the aspect of ecological informatics and not on the production and growth of fresh produce for sustainable production. On the other hand, EuroSpaceHub, ExoSpaceHab-X, and the Mobile Extreme Environment Research Station (MEERS) are key analog mission facilities that encompasses food production and autonomous vehicle testing; hence, they are highly expensive and not replicable for university-level research [23,24]. The European Space Agency's Large Centrifuge and the Centrifuge Rotor (CR) of the National Aeronautics and Space Administration (NASA) were made to operate from 0.01 *g* to 2 *g* more accurately [25]. Simulated gravity platforms, such as centrifuge-based platforms for growing agricultural and horticultural crops, are one of the great materializations of space analogs [26]. The current study is hinged upon improving the reliance of existing platforms to static light setups and single-axis clinostats that provide limited simulation fidelity, which constrains the exploration of dynamic plant responses to simultaneous stimuli. The majority of existing centrifuge-based platforms require the user to stop the experiment to check the growth of their plants; hence, it is addressed here through the integration of Cloud IoT technology (Figure 3). This study developed an Earth-based simulated partial gravity platform with seamless wireless environmental data transmission and monitoring and integrated aeroponic and lighting systems to support crop growth. Through this advanced information and communications technology, it would give an opportunity for researchers to monitor the growth of crops inside the centrifuge platform in real time. It can be extended by embedding models for vegetation index computations such as triangular vegetation index (TGI) and leaf pixels segmentation through lightweight machine learning algorithms and more advanced deep neural and transformer-based networks.

The R/S is a classical indicator of plant resource allocation strategy under environmental stress. Typically, under nutrient limitation, plants allocate more resources to root development to enhance mineral acquisition, resulting in an increased R/S ratio. Conversely, under low light intensity, plants often prioritize shoot elongation to improve light capture, leading to a decreased R/S ratio [13]. In our study, we observed a decline in R/S ratio under lower light intensities in both gravity conditions, which is consistent with this adaptive shift toward shoot development in light-limited environments. However, under simulated Martian gravity, the R/S ratio was generally lower than under Earth gravity, suggesting that mechanical unloading may have further altered biomass allocation patterns. This could be attributed to reduced gravitropic cues or energy partitioning differences in partial gravity analog conditions.

One limitation of the current study is that all replicates were conducted sequentially rather than simultaneously in multiple chambers. However, environmental variables such as temperature, humidity, and light intensity were tightly monitored and maintained across all runs to ensure reproducibility and minimize batch effects. The current setup lacks an active system for gas composition monitoring and control within the root zone. Oxygen and carbon dioxide solubility in the nutrient mist can vary depending on root zone temperature, mist droplet size, and pressure. These influence root respiration and metabolic activity [13]. Although passive aeration is partially achieved through intermittent misting and open chamber volume, future iterations of this platform would benefit from the inclusion of dissolved oxygen (DO) and CO_2 sensors, and possibly micro-bubblers or air injectors, to ensure consistent gas-phase regulation.

In the context of plant science, a longer root system provides greater surface area for the absorption of nutrients and minerals from the fertigation system during misting. In the context of limited space in space farming, especially the fabricated Earth-based clinostat, moderately longer roots are beneficial to avoid clogging the misters. Under microgravity, the amendment of growth simulators, such as indole acetic acid (IAA), gibberellic acid (GA), and ascorbate (AA), have been proven effective [27], but not in partial gravity environment as the case of the current study. Nonetheless, it should be considered that in aeroponic partial gravity environments, a slightly higher root-to-shoot ratio is beneficial for balanced adaptation. To deepen our understanding of root response mechanisms, future studies should examine root meristematic zones, cell polarity, and differentiation at the cellular level [28]. Overall, this study contributes to our understanding of gravitropic and phototropic responses in maize under partial gravity conditions. These findings inform future designs of bioregenerative life support systems (BLSSs) for space, where optimized root–shoot allocation is critical to sustainable food production.

A comparison among multiple studies of the effects of gravity on plant growth and the considered technologies is shown in Table 1, where only the developed clinostat has integrated Cloud-based monitoring. All in all, the developed triple-axis clinostat for Earth-based partial gravity simulation in growing green food aeroponically, with Cloud-based monitoring and automations in fertigation, is novel and impactful for future food generation. The Earth-based clinostat, such as the one developed in this study, successfully simulates partial gravity and light interactions relevant to Martian conditions; however, there are still several challenges present before having a direct translation of this technology to operational space agriculture. First, in actual Martian conditions, there is cosmic radiation, low atmospheric pressure, limited resource availability, and even thermal extremes that were not factored in the design of the currently developed clinostat. Second, long-duration exploration in space requires radiation-hardened materials unlike the acrylic and stainless steel materials used here. Third, although this study validates the initial biological response of maize through root and shoot length in relation to gravity–light interplay, CO_2 regulation, waste recycling, and continuous nutrient delivery are required to have a closed-loop bioregenerative life support system. And fourth, power constraints in space missions also pose limitations for the use of LED strips. Incorporation of additional space environmental stressors and scalability aspect is recommended for autonomous and long-duration cultivation systems. Hence, the developed three-axis clinostat supports scalable data logging for AI-driven phenotyping and adaptive control systems, is modular and allows custom modification for other crop types, and offers a biological benchmark for crop selection and genetic screening for future space missions.

Table 1. Comparison among multiple studies of the effects of gravity on plant growth and the technologies considered.

Platform/ Technology	Simulated Gravity (g)	No. of Rotating Axis	Grow Media	Wireless Connectivity	Type of Cultivation System	Crop of Interest	Root Zone Temperature (°C)	Light Spectrum	Ref.
Microgravity	0.02	2	Gel	None	Petri dish	*Arabidopsis thaliana*	22	Green	[8]
Partial gravity	0–0.9	2	Water	None	Petri dish	*Wolffia globosa*	Not specified	White	[6]
Partial gravity	0.17	3	Agar	None	Not specified	*Arabidopsis thaliana*	Not specified	White, red	[29]
Hypergravity	4	3	Agar	None	Well plates	*Wolffia globosa*	30.44 ± 1.24	340–820 nm	[30]
Hypergravity	5	1	Soil	IoT	Drip irrigation	*Zea mays* L.	21–31	RGB	[26]
Partial gravity	0.35–0.4	3	Foam	Cloud IoT	Aeroponic	*Zea mays* L.	23–29	RGB	This study

5. Conclusions

This study developed a Cloud-enabled triple-axis soilless clinostat for Earth-based simulation of partial gravity and light interaction in seedling tropisms. Finite element analysis confirmed the design structure and material to be applicable to withstand the potential strain, stress, and thermal hotspots and gradients during partial-gravity operation (0.35 g to 0.40 g) given a maximum of 10 kg grow chamber load at the center. Arduino UNO microcontroller boards were used to interface with temperature, humidity, moisture, light intensity, and gravity sensors and control the lighting, fertigation, and clinorotation systems. An Arduino ESP32 was used for Cloud IoT connectivity to ThingSpeak for continuous monitoring of enviro-physical parameters inside the grow chamber. Based on actual tests, the developed clinostat was proven to generate 0.252 g to 0.460 g inside the grow chamber that suits the target Martian gravity. The combined gravi-phototropic tests confirmed that maize seedlings exposed to partial gravity and grown using the aeroponic approach have a shoot system driven by light availability rather than gravity, which is the opposite for the root system. For future studies, it is recommended to develop other grow media to avoid the slow water absorption of horticultural foam, optimize integrated light and gravity control strategies for enhanced whole-plant growth, and explore other high-valued crops for cultivation.

Author Contributions: Conceptualization, C.R.C., J.C.D.C., M.C.L., C.L., J.J.V., R.C.II, and R.-J.R.; methodology, C.R.C., J.C.D.C., M.C.L., C.L., J.J.V., R.C.II, and R.-J.R.; software, C.R.C., J.C.D.C., M.C.L., C.L., and J.J.V.; validation, R.C.II, R.-J.R., and L.E.R.; formal analysis, C.R.C., J.C.D.C., M.C.L., C.L., J.J.V., R.C.II, R.-J.R., and L.E.R.; investigation, C.R.C., J.C.D.C., M.C.L., C.L., J.J.V., R.C.II, R.-J.R., and L.E.R.; resources, C.R.C., J.C.D.C., M.C.L., C.L., J.J.V., R.C.II, and R.-J.R.; data curation, C.R.C., J.C.D.C., M.C.L., C.L., J.J.V., R.C.II, and R.-J.R.; writing—original draft preparation, C.R.C., J.C.D.C., M.C.L., C.L., J.J.V., R.C.II, and R.-J.R.; writing—review and editing, C.R.C., J.C.D.C., M.C.L., C.L., J.J.V., R.C.II, R.-J.R., and L.E.R.; visualization, R.C.II and R.-J.R.; supervision, R.C.II; project administration, R.C.II; funding acquisition, R.C.II. All authors have read and agreed to the published version of the manuscript.

Funding: The APC was funded by De La Salle University Science Foundation.

Data Availability Statement: The raw data supporting the conclusions of this article will be made available by the authors on request.

Acknowledgments: This study is supported by the Office of the Vice President for Research and Innovation of De La Salle University, Manila, and the Department of Science and Technology-Engineering Research and Development for Technology (DOST-ERDT) Program of the Philippines.

Conflicts of Interest: The authors declare no conflicts of interest.

Abbreviations

The following abbreviations are used in this manuscript:

ASR	active surface ratio
AFP	air-filled porosity
AA	ascorbate
CNC	computer numerical control
CR	Centrifuge Rotor
CT	control treatment
EMCS	European Modular Cultivation System
FEA	Finite Element Analysis
GA	gibberellic acid
HI-SEAS	Hawaii Space Exploration Analog and Simulation

HSP	heat shock protein
IAA	indolic acetic acid
ISS	International Space Station
MDRS	Mars Desert Research Station
MEERS	Mobile Extreme Environment Research Station
PG	partial gravity
PWM	Pulse Width Modulator
RPMs	Random Positioning Machines
RGR	relative growth rate
WTT	water transport time
TGI	Triangular Greenness Index

References

1. Paul, A.; Wheeler, R.M.; Levine, H.G.; Ferl, R.J. Fundamental plant biology enabled by the space shuttle. *Am. J. Bot.* **2013**, *100*, 226–234. [CrossRef]
2. Perbal, G.; Driss-Ecole, D. Contributions of space experiments to the study of gravitropism. *J. Plant Growth Regul.* **2002**, *21*, 156–165. [CrossRef]
3. Morita, M.T. Directional gravity sensing in gravitropism. *Annu. Rev. Plant Biol.* **2010**, *61*, 705–720. [CrossRef]
4. Hughes, A.M.; Vandenbrink, J.P.; Kiss, J.Z. Efficacy of the random positioning machine as a terrestrial analogue to microgravity in studies of seedling phototropism. *Microgravity Sci. Technol.* **2023**, *35*, 43. [CrossRef]
5. Kiss, J.Z.; Millar, K.D.L.; Edelmann, R.E. Phototropism of Arabidopsis thaliana in microgravity and fractional gravity on the International Space Station. *Planta* **2012**, *236*, 635–645. [CrossRef]
6. Romano, L.E.; Van Loon, J.J.W.A.; Izzo, L.G.; Iovane, M.; Aronne, G. Effects of altered gravity on growth and morphology in Wolffia globosa: Implications for bioregenerative life support systems and space-based agriculture. *Sci. Rep.* **2024**, *14*, 410. [CrossRef]
7. Wang, H.; Li, X.; Krause, L.; Görög, M.; Schüler, O.; Hauslage, J.; Hemmersbach, R.; Kircher, S.; Lasok, H.; Haser, T.; et al. 2-D clinostat for simulated microgravity experiments with Arabidopsis seedlings. *Microgravity Sci. Technol.* **2015**, *28*, 59–66. [CrossRef]
8. Kim, S.M.; Kim, H.; Yang, D.; Park, J.; Park, R.; Namkoong, S.; Lee, J.I.; Choi, I.; Kim, H.-S.; Kim, H.; et al. An experimental and theoretical approach to optimize a three-dimensional clinostat for life science experiments. *Microgravity Sci. Technol.* **2016**, *29*, 97–106. [CrossRef]
9. Vandenbrink, J.P.; Herranz, R.; Medina, F.J.; Edelmann, R.E.; Kiss, J.Z. A novel blue-light phototropic response is revealed in roots of Arabidopsis thaliana in microgravity. *Planta* **2016**, *244*, 1201–1215. [CrossRef] [PubMed]
10. Porterfield, D.M. The biophysical limitations in physiological transport and exchange in plants grown in microgravity. *J. Plant Growth Regul.* **2002**, *21*, 177–190. [CrossRef] [PubMed]
11. Izzo, L.G.; Aronne, G. Root tropisms: New insights leading the growth direction of the hidden half. *Plants* **2021**, *10*, 220. [CrossRef]
12. Shen, Y.; Guo, S.; Zhao, P.; Wang, L.; Wang, X.; Li, J.; Bian, Q. Research on lettuce growth technology onboard Chinese Tiangong II Spacelab. *Acta Astronaut.* **2018**, *144*, 97–102. [CrossRef]
13. Hołtra, A.; Zamorska-Wojdyła, D. Assessment of the physiological condition of *Salvinia natans* L. exposed to copper(II) ions. *Environ. Prot. Eng.* **2015**, *41*, 147–158. [CrossRef]
14. Romano, L.E.; Iovane, M.; Izzo, L.G.; Aronne, G. A machine-learning method to assess growth patterns in plants of the family Lemnaceae. *Plants* **2022**, *11*, 1910. [CrossRef] [PubMed]
15. Kim, Y.J.; Jeong, A.J.; Kim, M.; Lee, C.; Ye, S.K.; Kim, S. Time-averaged simulated microgravity (taSMG) inhibits proliferation of lymphoma cells, L-540 and HDLM-2, using a 3D clinostat. *Biomed. Eng. Online* **2017**, *16*, 48. [CrossRef] [PubMed]
16. Kuya, N.; Nishijima, R.; Kitomi, Y.; Kawakatsu, T.; Uga, Y. Transcriptome profiles of rice roots under simulated microgravity conditions and following gravistimulation. *Front. Plant Sci.* **2023**, *14*, 1193042. [CrossRef]
17. Concepcion II, R.; Relano, R.J.; Janairo, A.G.; Francisco, K.; Garcia, L.; Montanvert, H. Effects of optimized interaction of short-term hypergravity stimulation and nitrate-deficient cultivation in maize root using genetic-immunological algorithms. *Plant Stress* **2024**, *14*, 100702. [CrossRef]
18. Attuluri, S.; Suman, S.; Srilatha, D.; Avasthi, V.; Singh, R. Monitoring and detecting plant diseases using cloud-based Internet of Things. *J. Electr. Syst.* **2024**, *20*, 183–194. [CrossRef]
19. Concepcion, R.; Ramirez, T.J.; Alejandrino, J.; Janairo, A.G.; Baun, J.J.; Francisco, K.; Relano, R.J.; Enriquez, M.L.; Bautista, M.G.; Vicerra, R.R.; et al. A look at the near future: Industry 5.0 boosts the potential of sustainable space agriculture. In Proceedings of the 2021 IEEE 13th International Conference on Humanoid, Nanotechnology, Information Technology, Communication and Control, Environment, and Management (HNICEM), Baguio, Philippines, 1 December 2022.

20. Relano, R.-J.S.; Francisco, K.G.; Concepcion, R.S.; Ducut, J.D.D.; Enriquez, M.L.C.; Vicerra, R.R.P.; Bandala, A.A.; Dadios, E.P. Tuber root growth in silico phenotyping using adaptive Neuro-Fuzzy Capacitive Resistivity Imaging system. In Proceedings of the 2022 7th International Conference on Business and Industrial Research (ICBIR), Bangkok, Thailand, 18 May 2023.
21. Dawson, S.J.; Roesch, J.E.; Solignac, A. Human factors studies for a Mars expedition. *Sci. Technol. Ser.* **2004**, *107*, 403–409.
22. Heinicke, C.; Poulet, L.; Dunn, J.; Meier, A. Crew self-organization and group-living habits during three autonomous, long-duration Mars analog missions. *Acta Astronaut.* **2021**, *182*, 160–178. [CrossRef]
23. Crotti, S.; Foing, B.; Pascual, J.; Puriene, V.; Zanchi, M. ExoSpaceHab-X: A transportable Moon base for analog missions & outreach. In Proceedings of the International Astronautical Congress(IAC), Baku, Azerbaijan, 2–6 October 2023.
24. Disher, T.J.; Anania, E.C.; Anglin, K.M.; Kring, J.P. Development of the mobile extreme environment research station (MEERS) analogue for usability and field testing of space technology. In Proceedings of the 29th Space Simulation Conference—"Fifty Years of Advancing the Testing Boundaries", Annapolis, MD, USA, 14–17 November 2016.
25. Nakano, T. The development of the International Space Station centrifuge. *Biol. Sci. Space* **2004**, *18*, 89–90.
26. Dionela, M.J.; Alaan, M.; Lato, J.R.; Reyes, J.; Tan, J.M.; Concepcion II, R.; Relano, R.J. Custom-Built Earth-Based Hypergravity Platform to Study Gravity and Light Tropisms on Soil-Grown Seedlings. *Appl. Sci. Eng. Prog.* **2025**, *18*, 1–15. [CrossRef]
27. Ikhajiagbe, B.; Anoliefo, G.O.; Orukpe, A.O.; Ibrahim, M.S. Effects of Selected Plant Growth Stimulators on Enhancing Germinability and Germination Parameters of *Zea mays* L. Under Microgravity Conditions Simulated by a Two-Dimensional Clinostat. *Int. J. Hortic. Sci. Technol.* **2023**, *10*, 1–10. [CrossRef]
28. Valbuena, M.A.; Mazano, A.; Vandenbrink, J.P.; Pereda-Loth, V.; Carnero-Diaz, E.; Edelmann, R.E.; Kiss, J.Z.; Herranz, R.; Medina, F.J. The combined effects of real or simulated microgravity and red-light photoactivation on plant root meristematic cells. *Planta* **2018**, *248*, 691–704. [CrossRef] [PubMed]
29. Medina, F.J.; Manzano, A.; Villacampa, A.; Ciska, M.; Herranz, R. Understanding Reduced Gravity Effects on Early Plant Development Before Attempting Life-Support Farming in the Moon and Mars. *Front. Astron. Space Sci.* **2021**, *8*, 729154. [CrossRef]
30. Romano, L.E.; van Loon, J.J.W.A.; Vincent-Bonnieu, S.; Aronne, G. Wolffia globosa, a novel crop species for protein production in space agriculture. *Sci. Rep.* **2024**, *14*, 27979. [CrossRef]

Disclaimer/Publisher's Note: The statements, opinions and data contained in all publications are solely those of the individual author(s) and contributor(s) and not of MDPI and/or the editor(s). MDPI and/or the editor(s) disclaim responsibility for any injury to people or property resulting from any ideas, methods, instructions or products referred to in the content.